Atmos. Meas. Tech. Discuss., 3, 1843–1860, 2010
www.atmos-meas-tech-discuss.net/3/1843/2010/

Atmospheric Measurement Techniques Discussions

On differentiating ground clutter and insect echoes from Doppler weather radars using archived data

S. J. Rennie[1], **A. J. Illingworth**[1], **and S. L. Dance**[1,2]

[1]Department of Meteorlogy, University of Reading, Reading, UK
[2]Department of Mathematics, University of Reading, Reading, UK

Received: 23 March 2010 – Accepted: 6 April 2010 – Published: 16 April 2010

Correspondence to: S. J. Rennie (s.j.rennie@reading.ac.uk)

Published by Copernicus Publications on behalf of the European Geosciences Union.

Abstract

Normally wind measurements from Doppler radars rely on the presence of rain. During fine weather, insects become a potential radar target for wind measurement. However, it is difficult to separate ground clutter and insect echoes when spectral or polarimetric methods are not available. Archived reflectivity and velocity data from repeated scans provide alternative methods. The probability of detection (POD) method, which maps areas with a persistent signal as ground clutter, is ineffective when most scans also contain persistent insect echoes. We developed a clutter detection method which maps the standard deviation of velocity (SDV) over a large number of scans, and can differentiate insects and ground clutter close to the radar. Beyond the range of persistent insect echoes, the POD method more thoroughly removes ground clutter. A new, pseudo-probability clutter map was created by combining the POD and SDV maps. The new map optimised ground clutter detection without removing insect echoes.

1 Introduction

Ground clutter is a major contaminant of weather radar scans. It is particularly obstructive when extracting comparatively weak insect echoes. Insects represent a potential Doppler radar target for wind measurement during fine weather. Normally Doppler radar wind observations for data assimilation in numerical weather prediction are only available from precipitation echoes, as is the case in the UK at present (N. Gaussiat, personal communication, 2010). Recent efforts to utilize insect echoes for wind observations have been hampered by the difficulty of removing ground clutter contamination (Rennie et al., 2010). Although target detection and clutter filtering can be accomplished using spectral analysis of the raw radar signal (e.g. Bachmann and Zrnić, 2008a; Hubbert et al., 2009a,b; Unal , 2009), such methods were not available when the utilization of insect echoes was explored. Therefore we sought to differentiate insect echoes and ground clutter using only reflectivity and velocity. Such a technique is also applicable to reanalysis of archives containing only the primary parameters (reflectivity (Z) and velocity (V)), or when no data from insect-free (*viz* winter) periods are available.

Many clutter detection methods for single polarisation radars have been used operationally (Alberoni et al., 2003; Meischner et al., 1997). “Simple” methods, such as mapping clutter using reflectivity, or identification by zero-velocity from Doppler radars, are being superseded by spectral methods and complex algorithms. There are recent examples of spectral techniques in the literature. For example, the UK Met Office produces a clutter indicator (*ci*) that describes the average pulse-to-pulse signal variability, which for “perfect” clutter should be 0 (Sugier et al., 2002). *Ci* can detect both ground clutter and anomalous propagation echoes (anaprop).

Another new clutter identification parameter, the Clutter Phase Alignment (CPA) (Hubbert et al., 2009a) is calculated as the ratio of the magnitude of the vector sum of the individual signal time series members divided by the sum of the magnitudes of the members. It has the advantage that it measures only phase changes and is unaffected by any variations in the power of the return. Improved clutter detection was achieved by combining CPA with the Clutter Mitigation Decision algorithm (Hubbert et al., 2009b; Ice et al., 2009). The latter is a fuzzy logic algorithm (for single or dual polarisation) which uses spectral and spatial characteristics.

In another example, Warde and Torres (2009) described a dynamic spectral method which utilises the high power and narrow spectral width of clutter, to optimally match the the ground clutter environment. Such dynamic methods have advantages over static clutter methods. However, the effectiveness of these methods must be reduced for weak signals where the ground clutter’s spectral characteristics are less representative. Bachmann and Zrnić (2008a) described a white clutter residue noise that obscured weak clear-air echoes. This noise remained after the near-zero velocity signals were removed, but could be filtered by further spectral analysis and filtering. Treatment of such a “noisy” clutter signal would be an important factor when removing ground clutter from amongst weak insect echoes.

Dual polarisation also offers a wide variety of methods (e.g. Friedrich et al., 2009; Gourley et al., 2007; Hurtado and Nehorai, 2008; Unal , 2009). Dual polarisation may also be used to discriminate airborne fauna (Bachmann and Zrnić, 2008b; Gauthreaux et al., 2008). The UK's first dual polarisation radar has been demonstrated to successfully discriminate insects and clutter (Rennie et al., 2008, 2010). Dual polarisation is more effective than single polarisation for identifying insects (e.g. Rennie et al., 2008) and also permits discrimination using only the data from individual scans.

The new clutter detection method described here arose from the endeavour to extract insect echoes from the UK C-band weather radar network (Rennie et al., 2010). During the field season for this work, the *ci* parameter mentioned above was produced by the UK Met Office for the long pulse scans only. It was apparent from the long pulse data that the *ci* of insects was much greater than zero, so *ci* has the potential for future insect/clutter discrimination. However, in the absence of the raw signal information or pre-processed spectral analysis, it was necessary to develop an alternative ground clutter detection method. The method used only reflectivity and velocity from archived scans. In this paper, Sect. 2 describes the radar data format and the general method for processing. Section 3 describes the development of two clutter detection methods, the probability of detection and the new standard deviation of velocity. In Sect. 4 these methods are appraised using an example and in Sect. 5 we propose an optimal solution for clutter detection based on the results.

2 Data and processing

There are four operational single-polarisation Doppler radars in the UK, from which data were collected during the summers of 2007 (Chenies only), 2008 and 2009. Three radars (Clee Hill, Cobbacombe and Dean Hill) have severe clutter that limits the area in which insects can be detected. Chenies has much less clutter, which is predominantly urban clutter because the radar is near London. The other radars' clutter results mostly from rural topography, which can be more difficult to detect due to non-stationary vegetation (Sugier et al., 2002).

The raw data comprise PPI (plan position indicator) conical scans that form a 2-D map around the radar, with dimensions of 360 1° rays by 167 range gates of 600 m. The elevations are nominally 1° 2° 4° 6° and 9°. To utilize insect returns, those sample volumes which contain insect echoes must be separated from those which contain ground clutter, birds, other types of contamination, or empty sample volumes. Precipitation echoes rarely coincide with insect echoes, and precipitation is also useful for wind observations. It may be supposed that a sample volume can contain a mixture of echo sources, especially farther from the radar as the beam spreads. Backscatter from side-lobes can also contribute targets "observed" within the sample volume. This makes target identification more difficult. A generic scheme for processing Doppler data is described below.

The first stage in processing is to exclude data from empty sample volumes, and from weak signals for which the user should not trust the velocity measurement. Noise from the amplifier will yield a constant signal that is observed in empty sample volumes. Removal of all weak signals can be accomplished by applying a threshold above this noise signal to ensure a minimum signal-to-noise ratio. Alternatively the threshold could be specified by the lower limit of reflectivity for whatever target is of interest, e.g. precipitation above 0 dB. It must also be noted that the radar detection threshold increases with range due to beam spreading.

Unreliable velocity measurements from weak signals or randomly-moving targets could alternatively be identified using signal parameters such as Doppler width, or a signal quality index (SQI). SQI as produced by the UK Met Office is defined as $|R_1|/R_0$, i.e. power normalized modulus of the autocorrelation at lag one (Doviak and Zrnić, 1984). In our experience, sample volumes excluded by either SQI or a suitable noise threshold are mostly coincident. The noise threshold option was used here because it did not require an additional parameter beyond Z and V.

The next stage is to remove the ground clutter, which would constitute the bulk of non-meteorological and non-biological returns. The amount of ground clutter can vary greatly among radars, depending on the radar location, surrounding topography, and suppression of side-lobes. In Sect. 1 a variety of techniques for identifying ground clutter was described, which utilise the characteristic motionlessness of the ground. The simplest method using only Z and V is to exclude near-zero velocities, but this removes valid insect or precipitation zero velocities and leaves too much ground clutter. In practice, ground clutter does not always give a consistent return. We found that sample volumes which were very likely clutter-affected, e.g. those with a signal above the detection threshold located at the periphery of regions that were obvious ground clutter, could register a speed as great as $10\,\mathrm{m\,s^{-1}}$. For this reason more discriminating methods were sought.

Final processing stages can include texture or Laplacian filtering, whereby large spatial changes in velocity or reflectivity between adjacent sample volumes indicate unreliable measurements. This final stage is important to filter out birds, aeroplanes or any other undesirable echoes, to ensure a wind product with minimal gross errors. We do not examine this further processing here.

3 Clutter detection methods

Two clutter detection methods, probability of detection and standard deviation of velocity, are described here. The variation of reflectivity over time was similarly explored, but proved less suitable so is not discussed here. Probability of detection is an established method (Alberoni et al., 2003) that uses accumulated counts over many scans, effectively creating a map of clutter.

3.1 Probability of detection (POD)

Probability of detection describes the frequency that a real target is detected within a sample volume. This may be determined from the frequency with which a sample volume returns a signal above a threshold, ideally the same threshold used to remove

AMTD

3, 1843–1860, 2010

empty sample volumes. Aggregated threshold exceedance over a period of many days to several months should indicate the ground clutter locations. The aggregate may be normalised to a value between 0 and 1, where 1 indicates 100% probability of clutter. Ideally the POD is created using scans close to the time of interest (e.g. recent months for contemporary scans). This reduces problems from ground clutter changing over time, such as with the seasons.

The POD characteristics for various targets are described below, assuming a threshold close to the noise limit.

- Ground clutter: generally high POD values. Lower values may be retrieved in marginal areas, e.g. where small changes in the beam propagation affect the presence of clutter echoes, or where the returned signal is at the threshold level.

- Precipitation: low POD values. Over a long period each sample volume will contain precipitation for only a small fraction of the time.

- Insects: insects normally occupy a shallow layer in the atmosphere, with distribution dependent upon the atmospheric conditions (e.g. Wood et al., 2009a,b). In the UK, from autumn to spring during dry weather, typically there are insect echoes within several hundred metres above ground level at all times of day and night, so a POD formed using data from summer will have a high value close to the radar.

- Birds: birds appear as random speckle, except during major migration periods, and will not contribute a high POD.

- Refraction: strong atmospheric refraction can reflect the signal back to the radar, or cause ground clutter or sea clutter to irregularly appear in some scans, i.e. anaprop. The POD will not detect this.

3.2 Standard deviation of velocity (SDV)

The variation in velocity at a location over an extended period of time provides a new clutter detection method. The standard deviation (std. dev.) of velocity calculated over many days should manifest different properties for different target types. Clutter should have the most constant velocity, noise will yield variable velocity, and precipitation is too transient to detect. Regions with omnipresent insects will yield a moderate std. dev. arising from the typical spread of wind velocities.

The std. dev. is calculated for each sample volume over repeated scans, to form a map of values. A computationally cheap method is proposed. The std. dev. σ is defined as the root mean square (RMS) of the difference between a value x_n and the mean, $\bar{x}$, i.e.,

$$\sigma = \sqrt{\frac{1}{N}\sum_{n=1}^{N}(x_n - \bar{x})^2}$$

where N is the number of samples, or in this context scans. However, by assuming that $\bar{x} = 0$, the calculation simplifies to the RMS of velocity over time, σ'. This assumption holds because (1) the mean velocity of noisy gates should be zero; (2) the mean velocity of stationary ground clutter should be zero; (3) the mean wind velocity over a long period of time should be zero; and (4) any other random targets should contribute a mean velocity of zero. (Regions with constant prevailing winds may require careful treatment.) In tests, the resulting σ' closely approximated the true σ.

The new standard deviation of velocity (SDV) parameter was created by converting σ' values into a pseudo-probability map, which makes it analogous to POD. (This choice is exploited later.) Empirically it was determined that $\sigma' > 7\,\mathrm{m\,s^{-1}}$ represented 0% probability of being clutter, and the minimum σ' (near 0) is 100% likely to be clutter. The pseudo-probability is calculated by: (1) SDV$= 7 - \sigma'$; (2) if SDV< 0 then set SDV$= 0$; (3) normalize SDV to be between 0 and 1 (divide the map of values by the maximum SDV value). Hence SDV= 1 is likely to be clutter just as POD= 1 is likely to be clutter.

4 Appraisal of methods

Here POD and SDV are applied, along with a noise threshold, to demonstrate their accuracy and functionality in separating insects and clutter. In practice, additional thresholds of Z and V may be considered in conjunction with these methods (e.g. Rennie et al., 2010).

The example chosen is from a cluttered radar (Clee Hill), which is located in England near the Welsh border. POD and SDV maps were created using archived radar data from summer. Then a scan was chosen from a day with good insect returns and a few showers: the 2° elevation scan on 29 June 2009 at 12:00 UTC. The radial velocity and reflectivity of the scan (Fig. 1) show a few showers to the north of the radar denoted by high Z and a clear radial velocity. The insect echoes are close to the radar, the red and blue of their velocity signal indicating northwestward travel. The ground clutter has high Z and is mostly situated close to the radar. Some spoking (azimuthal variation of noise) is apparent in the data; however this artefact does not affect the processing adversely.

As described in Sect. 2, a noise threshold should be applied first. The range-dependent noise threshold (NL) (also used to create POD) was calculated in reflectivity units of dBZ by

$$NL = 10\log_{10}(G(R-1)/200)^2 + I)$$

NL is the noise limit (threshold) at each range R in kilometres, G is the empirically-chosen gradient of the curve (5.5 for Clee Hill) and I is the y-intercept value which translates as the noise threshold at minimum range (in this case 0.001 resulting in an intercept at −30 dB). The range value used was nominally the start range of the pulse volume. NL in dB therefore increases non-linearly with range, being ≈ -8 dB at 20 km and ≈ 5.8 dB at 100 km in this case.

The following were applied to flag each sample volume in the scan.

1. All sample volumes with Z below the noise threshold are flagged as noise.

2. All areas where POD is greater than 0.5 are flagged as probable clutter.

3. All areas where the pseudo-probability SDV is greater than 0.5 are flagged as probable clutter.

In effect, one flag for weak signals and two for clutter have been applied sequentially. If these worked ideally, unflagged data would represent signal from insects or precipitation, and likely birds or other transient targets. The latter might be removed in subsequent processing stages, for example by using spatial filtering such as a Laplacian filter or despeckling algorithm.

The flag combinations for noise, POD and SDV are shown in Fig. 2. Most of the scan was flagged by the noise threshold (blue in Fig. 2), leaving regions where there were real targets (insects, precipitation, ground clutter, etc.). SDV and POD flagged similar regions (black), though POD was more comprehensive in identifying potential clutter far from the radar (red). Some sample volumes located at the edges of distant cluttered regions are flagged by both POD and noise (green, few sample volumes), indicating areas where the returned signal is probably often close to the noise threshold. The precipitation and insects, along with other real, transient targets, should have remained unflagged (white).

Close to the radar ($\approx$10 km range) there is a partial circle with only POD>0.5 (red) flags, due to omnipresent insects rather than ground clutter. This resulted from creating the POD using summer scans. The region near the radar flagged by SDV is more likely to really be ground clutter, as it matches the high Z regions in Fig. 1b. To demonstrate this, the velocity corresponding to several of these flag combinations is shown in Fig. 3.

AMTD

3, 1843–1860, 2010

Title Page
Abstract Introduction
Conclusions References
Tables Figures
◀◀ ▶▶
◀ ▶
Back Close
Full Screen / Esc
Printer-friendly Version
Interactive Discussion

The regions with no flag should ideally contain insects and precipitation, and no clutter. The velocity in unflagged (white) sample volumes (Fig. 3a) lacks areas with zero velocity due to clutter, which indicates successful clutter removal. Regions flagged as clutter by only POD, not SDV, (red flags) contain mostly clutter but also insects close to the radar, as evinced by the regions with velocity far from zero (Fig. 3b). Comparing Fig. 3 with 1a, SDV clearly differentiates the clutter and insects close to the radar much more effectively than POD.

5 Proposed solution

Optimal clutter detection should reflect SDV close to the radar and POD far from the radar. One solution is to combine POD and SDV into a new clutter map which is identical to SDV near the radar and identical to POD beyond the range of omnipresent insects. The transition occurs across the limit of insects affecting the POD. This is between the 14th and 25th range gates ($0.3 <\mathrm{POD}< 0.7$ in clutter-free regions near the radar) for Clee Hill at 2° elevation, corresponding to a range of ≈8 to ≈15 km. POD and SDV are combined with a range dependent, azimuthally uniform, weighting scheme W, where the new clutter map Cmap values are given by

$$\mathrm{Cmap}_i = \mathrm{POD}_i \cdot W_i + \mathrm{SDV}_i \cdot (1 - W_i)$$

for each sample volume i. W is set to 0 for the closest 14 ranges, increments by 0.1 between the 15th and 25th ranges, and remains at 1 out to the farthest range.

The results of applying a noise threshold and modified clutter map are shown (Fig. 4) using a Cmap threshold of 0.5. The velocity field of sample volumes not excluded by noise threshold or Cmap is extracted with little sign of clutter contamination (compare with Fig. 1a). A speckle filter or similar would be required to clean the velocity further and produce a suitable wind product. An upper reflectivity limit can also be applied at this stage, to distinguish precipitation from insects. Data processing should be optimised by careful choice of thresholds, and subsequent stringent speckle filtering.

This style of clutter map was used in processing all data in Rennie et al. (2010). The Doppler velocity was used to calculate VAD (velocity azimuth display, Browning and Wexler, 1968) wind profiles for comparison with model background wind profiles. Despite much effort in developing the processing procedure, results showed that clutter contamination still caused a low speed bias for highly cluttered radars (Rennie et al., 2010). In cases where the sample volumes containing ground clutter outnumber those containing insects, velocity observations are very sensitive to clutter contamination. Nevertheless, this method was the most successful in removing clutter while retaining insect echoes.

6 Conclusions

We have developed a method to separate ground clutter and insects using only velocity and reflectivity to create a pseudo-probability clutter map. Conventional probability of detection methods often fail to separate ground clutter from insects due to their omnipresence during summertime. When spectral or polarimetric methods are not available, the most effective way to distinguish insects and clutter close to the radar is to calculate the standard deviation of velocity over a long period of time, and convert the result into a pseudo-probability map. This can then be combined with a conventional probability of detection map, which is more effective at long ranges.

Acknowledgements. We thank the Met Office and BADC for provision and archive of the radar data. From the Met Office we acknowledge the assistance of Sue Ballard, Malcolm Kitchen, Nicolas Gaussiat, Tim Darlington, Robert Scovell and Jaqueline Sugier. This work is part of the FREE (Flood Risk from Extreme Events) Programme funded by NERC, grant NE/002137/1.

References

Alberoni, P. P., Ducrocq, V., Gregorič, G., Hasse, G., Holleman, I., Lindskog, M., Macpherson, B., Nuret, M., and Rossa, A.: Quality and assimilation of radar data for NWP – a review, COST717, http://www.shmi.se/cost717/doc/WDF_03_200104_1.pdf, 38 pp., 2003. 1845, 1848

Bachmann, S. and Zrnić, D.: Suppression of clutter residue in weather radar reveals birds' corridors over urban area, IEEE Geosci. Remote S., 5, 128–132, 2008a. 1844, 1845

Bachmann, S. and Zrnić, D.: Three-dimensional attributes of clear-air scatterers observed with the polarimetric weather radar, IEEE Geosci. Remote S., 5, 231–235, 2008b. 1846

Browning, K. A. and Wexler, R.: A determination of kinematic properties of a wind field using Doppler radar, J. Appl. Meteorol., 7, 105–113, 1968. 1854

Doviak, R. J. and Zrnić, D. S.: Doppler radar and weather observations, Academic Press, UK, 458 pp., 1984. 1847

Friedrich, K., Germann, U., and Tabary, P.: Influence of ground clutter contamination on polarimetric radar parameters, J. Atmos. Ocean. Tech., 26, 251–269, doi:10.1175/2008JTECHA1092.1, 2009. 1846

Gauthreaux Jr., S. A., Livingston. J. W., and Belser, C. G.: Detection and discrimination of fauna in the atmosphere using Doppler weather surveillance radar, Integr. Comp. Biol., 48, 12–23, 2008. 1846

Gourley, J. J., Tabary, P., and Parent du Chatalet, J.: A fuzzy logic algorithm for the separation of precipitating from nonprecipitating echoes using polarimetric radar observations, J. Atmos. Ocean. Tech., 24, 1439–1451, 2007. 1846

Hubbert, J. C., Dixon, M., Ellis, S. M., and Meymaris, G.: Weather radar ground clutter, Part I: Identification, modeling, and simulation, J. Atmos. Ocean. Tech., 26, 1165–1180, doi:10.1175/2009JTECHA1159.1, 2009a. 1844, 1845

Hubbert, J. C., Dixon, M., and Ellis, S. M.: Weather radar ground clutter Part II: Real-time identification and filtering, J. Atmos. Ocean. Tech., 26, 1181–1197, doi:10.1175/2009JTECHA1160.1, 2009b. 1844, 1845

Hurtado, M. and Nehorai, A.: Polarimetric detection of targets in heavy inhomogeneous clutter, IEEE T. Signal Proces., 56, 1349–1362, 2008. 1846

Ice, R. L., Rhoton, R. D., Krause, J. C., Saxion, D. S., Boydstun, O. E., Heck, A. K., Chrisman, J. N., Berkowitz, D. S., Zittel, W. D., and Warde, D. A.: Automatic clutter mitigation in the WSR-

88D, design, evaluation, and implementation, AMS 34th Conference on Radar Meteorology, Williamsburg VA, USA, 5–9 October 2009, P5.3, 2009. 1845

Meischner, P., Collier, C., Illingworth, A., Joss, J. and Randeu, W.: Advanced weather radar systems in Europe: The COST 75 Action, B. Am. Meteorol. Soc., 78, 1411–1431, 1997. 1845

Rennie, S. J., Illingworth, A. J., Dance, S. L., and Ballard, S. P.: Utilization of Doppler radar wind measurements from insect returns. Proceedings of ERAD 2008 – The Fifth European Conference on Radar in Meteorology and Hydrology, Helsinki, Finland, 30 June–4 July 2008, P2.6, 2008. 1846

Rennie, S. J., Illingworth, A. J., Dance, S. L. and Ballard, S. P.: Accuracy of Doppler radar velocities using insect returns, Meteorol. Appl., doi:10.1002/met.174, in press, 2010. 1844, 1846, 1851, 1854

Sugier, J., Parent du Châtelet, J., Roquain, P., and Smith, A.: Detection and removal of clutter and anaprop in radar data using a statistical scheme based on echo fluctuation, Proceedings of ERAD 2002 – The Second European Conference on Radar Meteorology, Delft, Netherlands, 18–22 November 2002, 17–24, 2002. 1845, 1847

Unal, C.: Spectral Polarimetric radar clutter suppression to enhance atmospheric echoes, J. Atmos. Ocean. Tech., 26, 1781–1797, doi:10.1175/2009JTECHA1170.1, 2009. 1844, 1846

Warde, D. A. and Torres, S. M.: Automatic detection and removal of ground clutter contamination on weather radars, AMS 34th Conference on Radar Meteorology, Williamsburg VA, USA, 5–9 October 2009, P10.11, 2009. 1845

Wood, C. R., O'Connor, E. J., Hurley, R. A., Reynolds, D. R. and Illingworth, A. J.: Cloud-radar observations of insects in the UK convective boundary layer, Meteorol. Appl., 16, 491–500, 2009a. 1849

Wood, C. R., Reynolds, D. R., Wells, P. M., Barlow, J. F., Woiwod, I. P. and Chapman, J. W.: Flight periodicity and the vertical distribution of high-altitude moth migration over southern Britain, B. Entomol. Res., 99, 525–535, 2009b.

1849

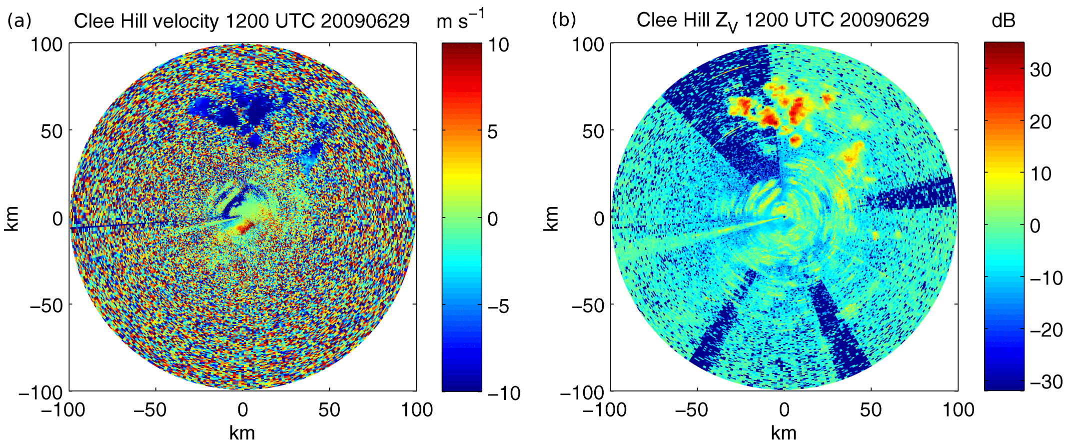

Fig. 1. Velocity and reflectivity of a 2° elevation scan from Clee Hill at 12:00 UTC on 29 July 2009. Insects, ground clutter and precipitation are visible.

AMTD
3, 1843–1860, 2010

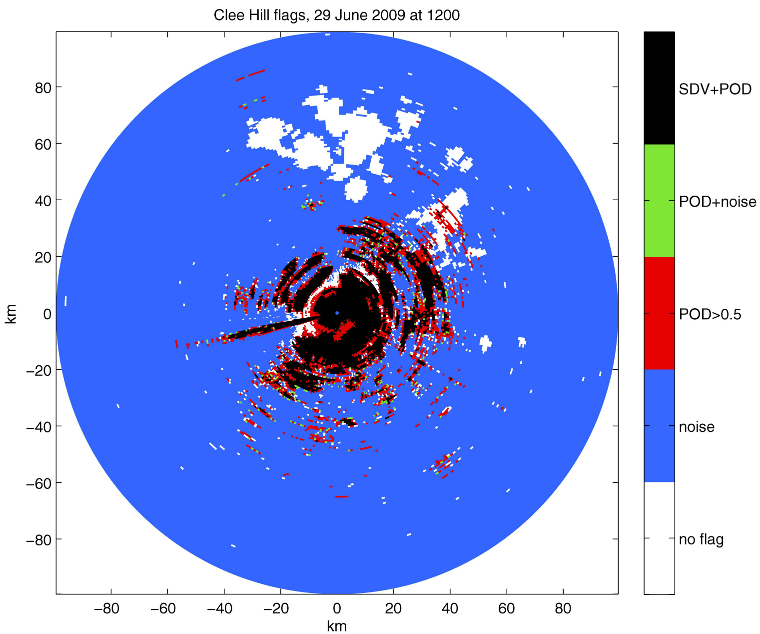

Fig. 2. Map of noise threshold, POD and SDV flags applied to the Clee Hill scan. The POD+noise flag combination is applied to few pixels. Real, non-clutter signals are unflagged.

AMTD
3, 1843–1860, 2010

On differentiating ground clutter and insect echoes

S. J. Rennie et al.

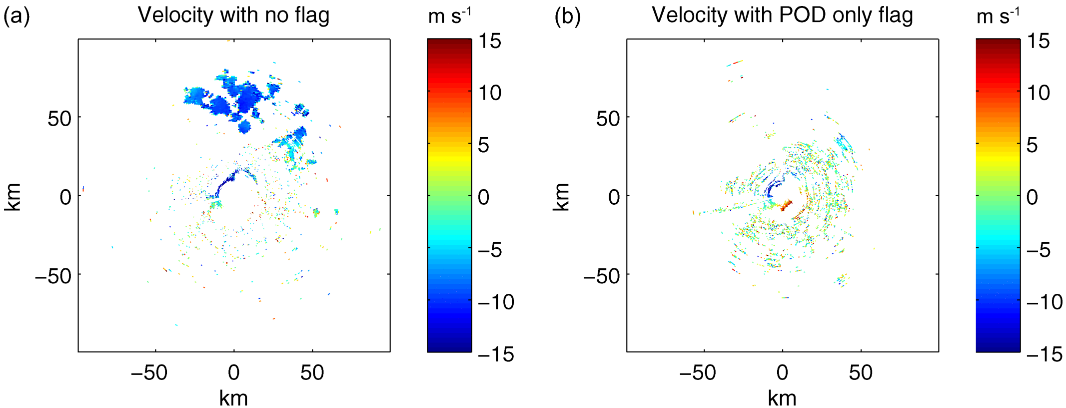

Fig. 3. (a) Velocity of areas with no flag in Fig. 2. **(b)** Velocity of areas flagged with POD only, including the insects near the radar visible as blue or red patches.

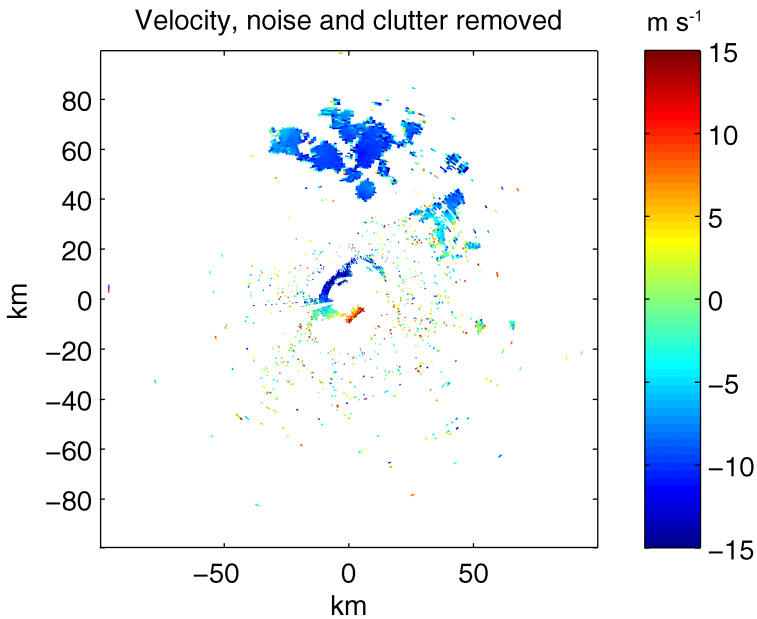

Fig. 4. Velocity data remaining after a noise threshold was applied and clutter removed using modified clutter map.

AMTD
3, 1843–1860, 2010

Title Page
Abstract
Introduction
Conclusions
References
Tables
Figures
◀
▶
Back
Close
Full Screen / Esc
Printer-friendly Version
Interactive Discussion